Fermi Surface Study of Spike Doped *GaAs* Superlattices

A. B. Henriques and S. M. Shibli
Instituto de Física, Universidade de São Paulo
Caixa Postal 20516, 01498 São Paulo, Brasil

Received July 12, 1993

We investigate the dependence of tlie Ferini surface on the doping period in periodically *Si* spike doped *GaAs*, for a doping period in the range 100-830Å. Tlie theoretical extremal cross sections of the Fermi surface are obtained from a self-consistent calculation of the miniband structure, whose comparison witli the experimental ones allows to cstimate the sheet carrier distribution in the superlattice minibands, thus providing a valuable means of sample characterization. The dependence of the Fermi surface upon the superlattice period pictures the crossover from two to three dimensional electronic structure. We also find evidence that the magnetic field induces tlie tunnelling of electrons between minibands, provided that the cgclotron energy is sufficiently liigh in comparison with the energy gap between tlie minibands. Photoconductivity spectra are described by an absorption threshold at tlie Fermi energy, which is pushed upwards when the superlattice period decreases.

I. Introduction

Spike doping is a technique which can be used to obtain carrier confinement in semiconductor microstructures. In Si spike doped *GaAs*, a sheet of *Si* donors is localized within a few monolayers of the crystal. The electrons, released from the shallow donors, are confined by a V-shaped space charge potential, a $\delta-$well. In a *$\delta-$superlattice, equally spaced dopant sheets* are introduced in the crystal, and the superposition of the V-shaped wells centered on different dopant slieets results in a periodic potential in one dimension, which gives rise to a miniband dispersion relation aiicl a Fermi surface. By varying tlie spacing between the dopant sheets, the strength of the interaction between adjacent $\delta-$wells can be tuned, and the system can be taken from a set of disconnected two dimensional systems for the widely spaced wells to an essentially anisotropic three dimensional system for the short period superlattice. The effect of coupling between adjacent wells when the superlattice period is made shorter can be investigated optical and magneto-transport studies of $\delta-$doped *GaAs*[1-4].

The electronic structure (minibands) for the $\delta-$superlattice can be calculated in the frame of the effective mass approximation[5], from which the theorctical interband emission and absorption spectra are obtained, and the main features detected experimentally are well reproduced. However, an interband optical spectrum requires the calculation of the valence band structure and a modelling of the bandgap renormalization, which is inherent to degenerate semiconductor systems, and these are unnecessary complications if one is interested in the energy spectrum for the conduction electrons only. An ideal test of the accuracy of the theoretical model for the conduction band structure (miniband widths, energy minigaps and position of the Fermi level) would be a direct comparison of tlie calculated electronic miniband structure with the experimental one, which is free from the difficulties related to tlie valence band and the renormalization of tlie bandgap. Such a test can be provided by the study of tlie Fermi surface of the $\delta-$superlattice, which is the object of the present report.

II. Experimental

The samples were grown on (100) GaAs undoped semi-insulating substrates in a Varian GEN II MBE

system. A ratio of As_4 and Ga beam equivalent pressures around 20 was chosen. The substrate temperature was 540^oC, which was determined with an Ircon V - series pyrometer, with tlie emissivity sct. at 0.70. These growth conditions ensure a (2 x 4) As stabilized surface reconstruction during MBE growth. In all samples, a MBE undoped $GaAs$ buffer layer was grown before doping. Tlie growth rate for MBE was estimated to be 1.5 $\mu m/h$. According to these growth rates, the layer spacing was estimated, which mas varied from 830Å down to 100Å, while the doping level per period was kept constant at approximately 3.0 x $10^{12} cm^{-2}$.

The Shubnikov–de Haas oscillations were studied at a fixed temperature of $T = 2\ K$ in magnetic fields up to 9 T. The sample holder allowed for rotation of the sample, and the direction of the magnetic field relative to tlie superlattice axis was established with an accuracy better than 0.1^o. The samples were illuminated with a red LED before measurements were started. Hall measurements at $2\ K$ mere performed using the van der Pauw technique, and the average Hall mobility was approximately $4000 cm^2/Vs$ for all samples. Photoconductivity measurements were performed ai a. sample temperature of $2\ K$. Light from a tungsten lamp was dispersed by a grating monochromator and conveyed to the sample by an optical fibre bundle.

III. Rcsults and discussion

For all tilt angles (the angle between the magnetic field directioi· and the superlattice axis), the magnetoresistance displays oscillatory components, which are periotlic in inverse field.

First tlie transverse SdH spectra (field applied parallel to tlie growth direction) will be discussed. Fig. 1 shows the inverse field Fourier transform for samples with a superlattice period ill the range 830Å–100Å. For the 830Å sample, the δ–wells are disconnected, and three peaks are detected, which correspond to tlie occupancy of three subbands. The occupancy of the ground-state ($E1$) miniband, which contains most of the electronic charge, is detected only as a weak peak in the Fourier spectrum, which is because of its relatively lower mobility due to the strong localization, or short binding length, of the $E1$ electrons[6]. When tlie δ–well spacing is decreased, the binding length rises, and so does the relative strength of the peaks related to the ground-state miniband occupancy; simultaneously, tlie widths of the minibands increase, while the number of populated minibands is reduced. For the 100Å sample, most of the electrons are in the ground-state miniband, which gives rise to a strong peak in the high frequency range of the Fourier spectrum.

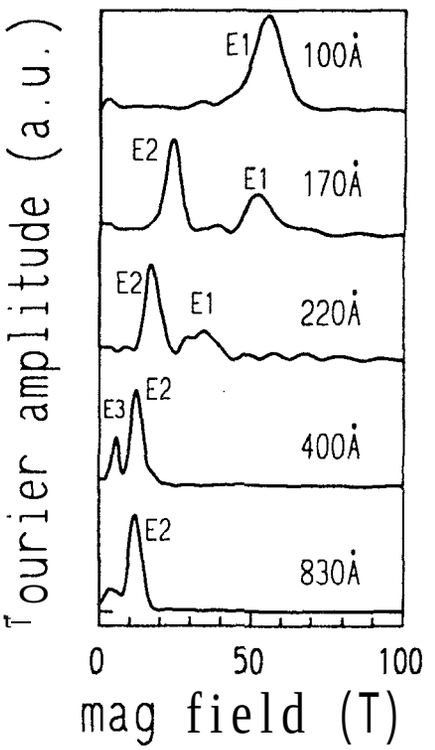

Figure 1: Fourier spectia of the experimental recordings of tlie inverse field Shubnikov-de Haas oscillations. The nominal spacing between tlie 6–wells for each curve is indicated. The miniband corresponding to each peak is indicated.

The peaks B_i in the Fourier spectra are the extremal cross sections A_i of the Fermi surface in a plane perpendicular to the field direction, in units of $\hbar/2\pi e$. This hypothesis is exactly true in tlie semi–classical limit (at a high Landau level filling factor), but also remains as a very good approximation in the vicinity of the quantum limit for an electron gas in a one–dimensional potential, as can be demonstrated by numerical calculations[7]. In order to interpret quantitatively the SdH data, it is necessary to know the shape of the Fermi surface, which

we calculated self-consistently. The self-consistent procedure included the conduction band non-parabolicity and the exchange-correlation correction in the local density approximation. The input parameters were the superlattice period and the sheet carrier density per period. Details of the calculation procedure are given elsewhere[5].

The Fermi surface has the growth direction as its axis of symmetry, and can be represented by its rotationally symmetric cross section. The Fermi surface for the 100Å superlattice is shown in Fig. 2 in the extended zone scheme. The outer curve, recognized as a cylinder with a periodically modulated cross-section, is the Fermi surface for the $E1$ miniband, whereas the next miniband ($E2$) gives the lens-shaped surface centered around the minizone extremum.

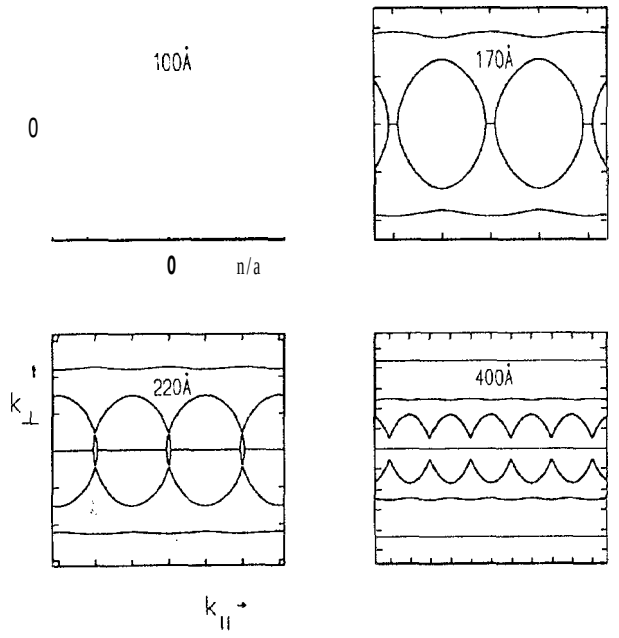

Figure 2: Cross section of the Fermi surface of a δ−superlattice in a plane containing the growth axis. The divisions on the axes are in units of π/a (a is the superlattice period, indicated for each structure). All figures enclose the same area of momentum space.

If the superlattice period is increased, the Fermi surface for the second miniband swells until it opens at the center of the Brillouin zone, thus changing gradually from the lens-like shape to the periodically modulated cylinder one; when the superlattice period is increased further, the third miniband (E3) starts to be populated, which gives rise to a new Fermi lens-like surface at the minizone center, as for the 220Å superlattice, also shown in Fig. 2. Conversely, if the superlattice period is reduced from 100Å, electrons are transferred from the second to the first miniband, whose Fermi surface becomes more strongly modulated, and ultimately becomes closed.

The electronic minibands described by an open Fermi surface will contribute to the transverse SdH oscillations with a 'belly' and a 'neck' frequency, (which become degenerate in the uncoupled δ−well limit), while the minibands described by a closed Fermi surface will be characterized by a single frequency.

For an open (cylinder-like) Fermi surface, the extremal cross section in a plane perpendicular to the field direction will increase when the direction of the magnetic field is tilted, and will be finite only below a critical tilt angle, θ_c, above which only open orbits in k−space are allowed. For a closed (lens-like) Fermi surface, the cross-section decreases when the field is tilted. These opposite tendencies can be observed in Fig. 3, which shows the Fourier transform of the SdH spectra evolution as a function of the angle between the growth direction and the magnetic field (0). For the 170Å and the 220Å samples, a strong peak at low frequencies is displaced to the left when θ increases, whereas a weak peak at high frequency moves to the right. The low frequency peak corresponds to a partially filled second miniband, and the high frequency one is due to a filled ground-state miniband. For the 400Å structure, two peaks are detected at low frequencies; the lower frequency one, which is displaced to the left one the sample is tilted, is ascribed to a partially filled E3 minihand, and the one that moves to the right is ascribed to a full $E2$ miniband. In the 830Å period structure, the peak positions scale as $\cos\theta$, as expected for a set of disconnected 2D systems. The 100Å structure shows a single peak of constant frequency, which is indicative of a 3D electronic structure.

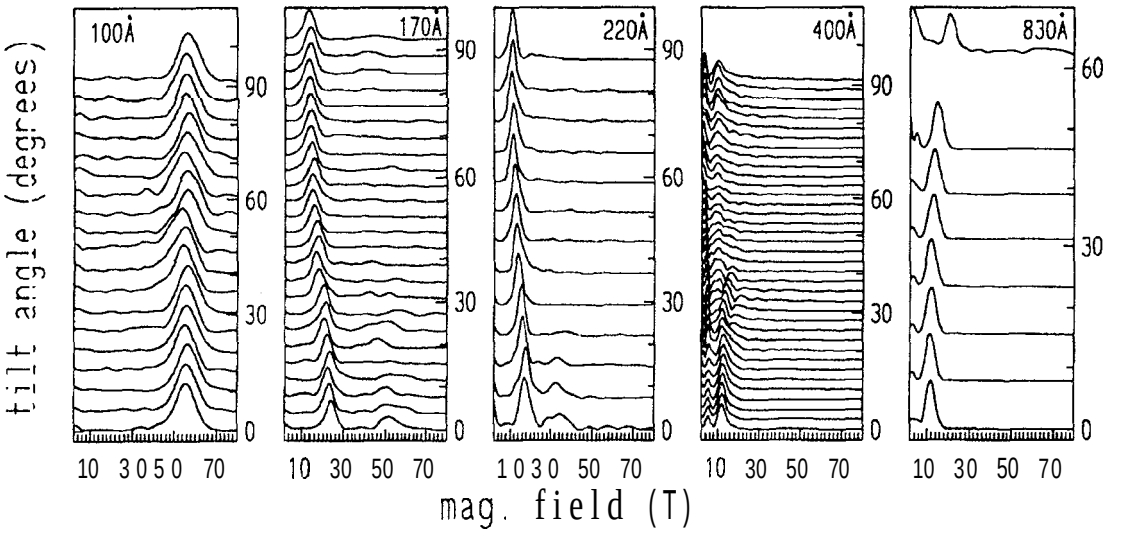

Figure 3: Fourier transform oii the inverse field Shubnikov de Haas oscillations. Tlie tilt angle to each curve is obtained by following the spectrum baseline to the right side. The spacing between tlie δ–wells, correspondent to each set of curves, is indicated.

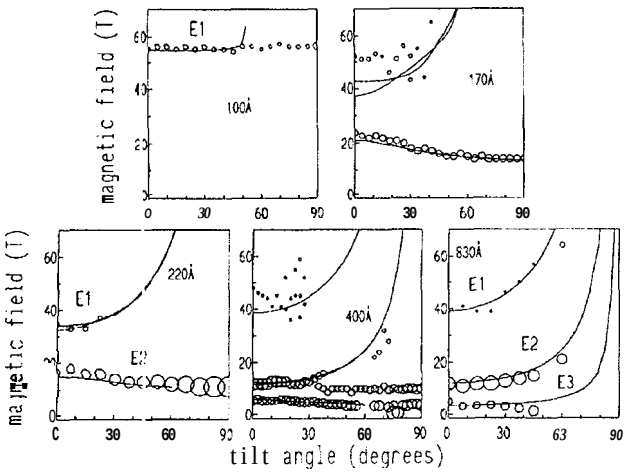

Figure 4: Open circles show the frequencies B_i, obtained froin the Fourier spectra of Fig. 3. The area of each circle is a measure of the relative intensity of the Fourier peak. Solid lines are the Fermi surface cross sections, obtained from the numerical calculations.

The angular dependence of the peak positions detected in the spectra of Fig. 3 is shown by dots in Fig. 4. The radius of each dot is a measure of the relative intensity of the corresponding peak; the general trend observed for all samples is that when tlic peak moves to higher frequencies as the tilt angle increases, its amplitude fades oiit rapidly. This effect is due to an increasing cyclotron mass with the tilt angle. As the sample is tilted, the quantization condition, $\omega\tau_Q > 1$, where τ_Q is the quantum lifetime, is reached progressively weaker in the range of fields of our experiments, leading to weaker oscillations. Conversely, for the electronic orbits in the lens-like sections of the Fermi surface, the cyclotron mass decreases, and tlie amplitude of the SdH increases.

In the numerical calculations, the superlattice period was taken as equal to the nominal value, and the total sheet carrier density, n_s, was adjusted to obtain the best agreement between the calculated extremal cross sections of the Fermi surface and the frequencies (B_i) for $\theta = 0$. For the samples studied, we find n_s to be in a range of 2.2 – 2.8 x $10^{12} cm^{-2}$, which is reasonably close to tlie intended doping level. With the input parameters thus fixed, the extremal cross sections of the Fermi surfaces were calculated for tlie whole tilt angle interval (0 – 00").

The calculated Fermi surface extremal cross section dependence oii θ closely match the measured frequencies B_i, however, for some of the samples, described by an open Fermi surface, agreement is only obtained below the critical tilt angle θ_c. Most noticeahly, this is the case for the $E1$ Fermi surface cross section of

Table 1: Estimated magnetic field (Tesla) required for the breakdown of Bragg reflection of the electrons in tlie $E1$, E2 and $E3$ minibands.

Superlattice period	E1	E2	E3
100Å	1.7^{ab}	–	–
170Å	5.9	–	–
220Å	8.5	$< 1.0^{ab}$	–
400Å	16.6	4.8	5.0^{b}

[a] Breakdown expected from $\hbar w_c E_F >$ A'
[b] Experimental points persist above $\mathbb{R}_{,}$

the 100Å superlattice (O, $\sim 50^0$), the E2 of the 220Å one (O, $\sim 60^0$), and the E3 of the 400Å superlattice (0, $\sim 60^0$). Above these 0,, whereas no finite extremal cross-sections for the corresponding Fermi surface miniband exist, tlie experimental curve persists.

The appearance of frequencies above tlie critical angle can occur as the result of magnetic breakdown of the Bragg reflections by tlic superlattice planes. Tlie magnetic field strength required foi an electron to cross a Bragg plane and transit between two minibands, separated by a gap of energy Δ, is $\hbar w_c E_F > \Delta^2$, where w_c is the cyclotron frequency and E_F is the Fermi energy. The calculated magnetic fields required for tlie breakdown of Bragg reflection are shown in Table 1, and are clearly consistent with tlie hypothesis of magnetic breakdown. However, this is still only an indirect evidence of its occurrence; a direct observation (by employing stronger magnetic fields than the ones used in this work) would be a more accurate test of this hypothesis and therefore of the accuracy of the theoretical calculations.

The photoconductivity spectra. at 2K for tlie 170, 220 and 400Å $\delta-$superlattices in the energy range near the $GaAs$ band-edge were measured, and are sliown in Fig. 5. Tlie spectra are described by a smooth absorption onset, which blue shifts when the superlattice period decreases; this is a consequence of tlie increase of tlie Fermi energy[5]. Tlie theoretical threshold for absorption from the n-th hole miniband, indicated by arrows in Fig. 5, was estimated by

$$h\nu_{\text{threshold}} = E_G + BGR - V_0 + E_F + H_{nF}$$

where $E_G = 1.519\ eV$, V_0 is the potential barrier between tlie wells, E_F is the Fermi energy measured from tlie bottom of tlie well, H_{nF} is the hole energy a.t the Fermi wave vector, and $BGR \sim -34$ meV, as estimated for a 3D electron gas[8].

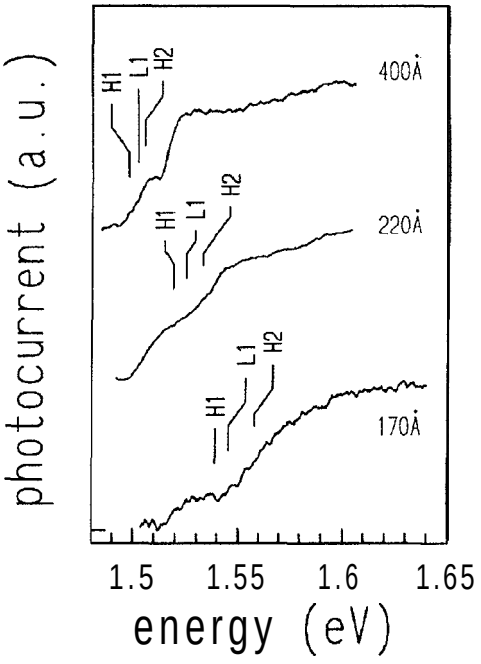

Figure 5: Photoconductivity spectra of periodically spike doped $GaAs$. Tlie spacing between tlie $\delta-$wells is indicated for each curve. Theoretical transition thresholds are indicated by arrows.

In summary, we have studied the magnetoresistance oscillations in $GaAs$ $\delta-$superlattices in tilted magnetic fields. These can be interpreted in terms of the shape of the Fermi surface, which evolves progressively from tlie cylindrical sliape in the uncoupled 6–well limit, and approaches a sphere for tlie short period superlattices, and for a doping period below 100Å the electronic structure is effectively three-dimensional. It is shown that the occurrence of magnetic breakdown of Bragg reflection is a probable effect in these systems, and its study can provide an important test of the accuracy of the theoretical modelling of the conduction band structure. Photocon-

ductivity spectra were also measured, and tlie spectra obtained are consistent with the interpretation of the transport data. A complication whose importance remains to be investigated is the effect of magnetic depopulation of tlie minibands[9]. Iii addition, we have not examined a possible influence of tlie incident light upon the self-consistent potential for electrons and holes[10] in tlie interpretation of the optical measurements.

Acknowleclgements

This work is supported by tlie FAPESP Grant No. 91/3336–9 and the CNPq Grant No.306335/88.

References

1. F. Koch, A. Zrenner and M.Zachau, in *Two-Dimensional Systems: Physics and New Devices* edited by G. Bauer, F. Kuchar, H. Heinrich (Springer–Verlag, Berlin, 1986) p.175.
2. R. Drcopad, S. D. Parker, E. Skuras, R. A. Stradling, R. L. Williams, R. R. Beall and J. J. Harris, in *High Magnetic Fields in Semiconductor Physics II* edited by G. Landwehr (Springer–Verlag, Berlin, 1989) p.199.
3. A. C. Maciel, M. Tatham, J. F. Ryan, J. M. Worlock, R. E. Nahory, J. P. Karbison and L. T. Florez, Surf. Sci. **228,** 251 (1990).
4. Mao-Long Ke, J. S. Rimmer, B. Hamilton, J. H. Evans, RI. Missous, K. E. Singer and P. Zalm, Pliys. Rev. B 45, 14114 (1992).
5. A. R. Henriques and L. C. D. Gonçalves, Sem.Sci.Technol. **8**, 585 (1993).
6. S. Yamada and T. Makimoto, Appl. Phys. Lett. **57**, 1022 (1090).
7. A. B. Henriques (1993), unpublished.
8. S. das Sarma, R. Jalabert and S. R. E. Yang, Phys. Rev. B 41, 8288 (1990).
9. A. Zrenner, H. Reisinger, F. Koch, K. Ploog and J. C. Maan, Phys. Rev. B **33,** 5607 (1986).
10. B. Ulrich, C. Zhang and K. v. Klitzing, Appl. Phys. Lett. 54, 1133 (1989).